


Whole-body MRI Quantification for Assessment of Bone Lesions in Chronic Nonbacterial Osteomyelitis Patients Treated With Pamidronate: A Prevalence, Reproducibility, and Responsiveness Study

Jyoti Panwar¹ , Mirkamal Tolend², Lillian Lim³, Shirley M. Tse⁴, Andrea S. Doria², Ronald M. Laxer⁴, and Jennifer Stimec²

ABSTRACT. *Objective.* The purpose of this study was (1) to assess the interreader reliability in detecting and scoring the inflammatory bone lesions in pediatric patients with chronic nonbacterial osteomyelitis (CNO) by using whole-body magnetic resonance imaging (WB-MRI), and (2) to evaluate the responsiveness of the MRI-detected CNO lesions to pamidronate therapy.

Methods. Eighty-eight WB-MRI examinations were independently reviewed and scored by 2 radiologists blinded to clinical details in 32 retrospectively enrolled pediatric patients with CNO. Inflammatory bone lesions, soft tissue abnormality, and bony structural changes were scored before and after pamidronate therapy. Lesion responsiveness was calculated by using standardized response mean and interreader reliability was assessed by k statistics.

Results. There was good to excellent interreader agreement for the detection and quantification of bone lesions. After the first cycle of pamidronate in all 32 patients, 96 of the 279 lesions (34%; after excluding 108 lesions of hand and feet) resolved, whereas in a subset of 11 patients with 2 or more cycles, 76% of lesions resolved after the second cycle. Twenty-one (7.5%) lesions worsened and 46 (16.4%) new lesions developed after 1 cycle in all 32 patients. In these 11 patients, the number of worsened lesions reduced to 2 (2%) and new lesions to 14 (14.9%) after the second cycle as detected on MRI. Vertebral lesions had the highest response to treatment.

Conclusion. WB-MRI is a reliable tool for objective quantification and assessment of response to treatment of pediatric CNO bone lesions and could be used to monitor disease activity for clinical and research purposes.

Key Indexing Terms: chronic nonbacterial osteomyelitis, magnetic resonance imaging, pamidronate, reliability/reproducibility of results, responsiveness, scoring system

¹J. Panwar, MD, FRCR, Department of Radiodiagnosis, Christian Medical College and Hospital, Vellore, India and Department of Diagnostic Imaging, The Hospital for Sick Children, Department of Medical Imaging, University of Toronto, Toronto, Ontario; ²M. Tolend, BSc, A.S. Doria, MD, PhD, MSc, MBA, J. Stimec, MD, FRCPC, Department of Diagnostic Imaging, The Hospital for Sick Children, Department of Medical Imaging, University of Toronto, Toronto, Ontario; ³L. Lim, MD, FRCPC, Division of Pediatric Rheumatology, Department of Pediatrics, University of Alberta, Edmonton, Alberta; ⁴S.M. Tse, MD, FRCPC, R.M. Laxer, MDCM, FRCPC, Division of Rheumatology, The Hospital for Sick Children, University of Toronto, Toronto, Ontario, Canada.

The authors declare no conflicts of interest.

Address correspondence to Dr. J. Panwar, Department of Radiodiagnosis, Christian Medical College and Hospital, Vellore 632004, India, and Department of Diagnostic Imaging, The Hospital for Sick Children, Department of Medical Imaging, University of Toronto, Toronto, ON M5G 1X8, Canada. Email: drjyotimcb@gmail.com, jyoti.panwar@sickkids.ca.

Accepted for publication September 5, 2020.

Chronic nonbacterial osteomyelitis (CNO), also known as chronic recurrent multifocal osteomyelitis (CRMO), is a rare inflammatory bone disorder characterized by relapsing and remitting aseptic bone lesions^{1,2}. It occurs primarily in children and adolescents who present with recurrent nonspecific osseous pain and swelling, and may sometimes be associated with systemic symptoms such as fever, weight loss, and generalized malaise^{3,4}. The median age of disease onset is 10 years with a predilection for females⁵. The etiology remains unclear and it is presumed to be an autoinflammatory disorder^{2,6}. It can be associated with SAPHO (synovitis, acne, pustulosis, hyperostosis, osteitis) syndrome⁶, inflammatory bowel disease⁷, psoriasis⁸, and sacroiliitis^{9,10}. CNO usually affects the metaphysis of tubular bones, mainly the lower extremities, followed by the clavicle and spine^{11,12,13}. Several imaging methods can be used to assess CNO lesions including radiographs, computed tomography, magnetic resonance imaging (MRI), and bone scintigraphy^{14,15}.

MRI is more sensitive than radiographs in the early detection of bone and soft tissue inflammatory lesions of CNO, which is important for diagnosis and institution of appropriate management to ensure improved patient outcomes and quality of life¹⁶.

Approximately 80% of patients respond to treatment with nonsteroidal antiinflammatory drugs (NSAID)^{17,18,19} and the remainder may be treated with second-line therapy including sulfasalazine, methotrexate^{17,19}, corticosteroids^{17,19}, bisphosphonates^{20,21}, and biologic agents^{18,21,22}. Fluid-sensitive, fat-saturated whole-body (WB)-MRI sequences are highly sensitive and specific in demonstrating active disease along with the extent of the lesions and are proven to be very effective for initial and follow-up diagnostics for children with CNO^{23,24,25,26}. There have only been a few studies that have evaluated the treatment response of patients with CNO on WB-MRI^{26,27,28,29,30,31} or the efficacy of pamidronate as second-line therapy of CNO^{27,28,29,30,31}. Despite the frequent application of WB-MRI in the assessment of CNO lesions, there is only 1 previous consensus-driven study published regarding the comprehensive quantification of disease by scoring these bone lesions and evaluating the interrater reliability³². There is no published study comparing the total skeleton disease load pre- and posttreatment by using the WB-MRI grading and scoring system. Hence, this study attempted to evaluate the interobserver reliability and to assess the response to pamidronate in pediatric CNO by utilizing the WB-MRI quantification system.

MATERIALS AND METHODS

This retrospective study was undertaken at a large pediatric quaternary care referral center and approved by the institutional research ethics board (No. 1000044463). The consent from all patients was waived owing to the retrospective features of the study. WB-MRI is a routine investigation at our institution, utilized for initial diagnosis and follow-ups to evaluate the effect of drug therapy on pediatric CNO lesions.

Patient selection. The patients identified and included in the study were all < 18 years, had a clinical (fulfilling the Bristol Criteria)^{33,34} and/or biopsy-proven diagnosis of CNO, were followed in the Rheumatology Clinic at The Hospital for Sick Children, and underwent pre- and post-pamidronate WB-MRI examinations within a period of 12 months from May 2010 to June 2017. WB-MRI were obtained before and after completion of each cycle of pamidronate infusions. Children whose symptoms failed to be controlled with NSAID for at least 1 month were treated with intravenous pamidronate at a dose of 1 mg/kg/day (maximum 60 mg/day) once per month for 3 months. Some patients were treated with additional cycles depending on clinical and radiographic responses. If the response to pamidronate was suboptimal or in the presence of a disease flare, patients were then switched to a tumor necrosis factor (TNF) blocker [either adalimumab (ADA) or etanercept (ETN)]. A total of 88 WB-MRI studies were analyzed in the 32 patients included in the study. Eleven patients received > 1 cycle of pamidronate treatment and thus completed > 1 follow-up MRI examination (Supplementary Figure 1, available with the online version of this article). All the posttreatment MRI were done at an average period of 5 months after each cycle of pamidronate therapy. Demographic, pre- and posttreatment clinical, relevant laboratory data, and other therapy details were retrieved from our electronic database.

MRI protocol. All MRI studies were performed on a 1.5-T MRI system (Magnetom Avanto, Siemens), with a "WB-MRI CRMO" institutional protocol used for the evaluation of CRMO. All examinations were performed with a dedicated multichannel surface coil system, with the

patient in the supine position and their hands being held by the side of their body. The integrated multichannel surface coil system allowed for the contiguous scanning. All exams included T2 single short-tau inversion recovery (STIR) coronal sequences at multiple stations covering the whole body from vertex to toes with the patient free-breathing. The coronal T2 STIR sequence was performed with the following variables: repetition time (TR) 3000 ms, echo time (TE) 60 ms, inversion time (TI) 165 ms, field of view (FOV) 400–500 mm, matrix 380 × 290, slice thickness 5 mm with 1-mm gap, number of signal averages (NEX) 6, echo train length (ETL) 26, and pixel bandwidth 446 Hz. The approximate scan time for each station was 5 min. The T2 STIR sagittal sequence of the spine was acquired at 2 stations and the time for each station was 5 min. The total scan time varied from 35 to 40 min depending on the child's height.

MRI assessment. Before the study, 2 pediatric musculoskeletal (MSK) radiologists (JS and JP) with > 5 years of experience in reading MSK MRI were familiarized with the MRI scoring protocol in a trial involving 10 patients who were not part of the study. Both the MSK radiologists are also members of an international CNO working group. Each radiologist independently interpreted and scored the MRI using a standard picture archiving and communication system (PACS) workstation (GE Medical Solutions) in random order, blinded to clinical and treatment details.

Selection of anatomical locations for assessment. We grouped the locations into the head (skull and mandible), shoulder girdle (clavicle and scapula), thorax (sternum and ribs), upper (humerus, radius, and ulna) and lower (femur, tibia, and fibula) extremities, hand (carpals, metacarpals, and phalanges), feet (tarsals, metatarsals, and phalanges), pelvis (ilium, sacrum, coccyx, periacetabulum, and ischium and/or pubis) and spine (from C1 to L5 vertebrae). For scoring purposes, all the long tubular bones of the upper and lower limbs were divided into 3 main regions: proximal epimetaphysis, diaphysis, and distal epimetaphysis. The lesions of the bones of the hands and feet were counted and scored by the number of involved bones. The head region (consisting of the right and left halves of the skull and mandible), shoulder girdle (including each side of the clavicle and scapula), right- and left-sided ribs, sternum, vertebrae from C1 to L5, and each side of the sacrum and iliac bones, coccyx, right and left-sided periacetabular, and ischium and/or pubis bone segments (considered as one region) were scored. Additionally, the presence and absence of the involvement of the posterior element of the spine was recorded and scored.

Definitions and grading of item selection for the selected locations. The diagnostic item selections and definitions were decided based on the previously published MRI-based definitions in CNO and the Spondyloarthritis Research Consortium of Canada scoring system for sacroiliitis studies^{26,27,35,36}. Bone lesions were defined as abnormal hyperintensity of the bone marrow on STIR images compared to surrounding normal marrow. The presence of hyperintensity in the surrounding soft tissue was also recorded as soft tissue inflammation. Bone marrow signal size, signal intensity, adjacent soft tissue high signal, and bone expansion were selected as the key pathologic items for scoring the CNO lesions. Images were evaluated for the presence of focal, high-signal intensity in all STIR sequences. Subsequently, these marrow signal abnormalities at all the relevant anatomic locations were analyzed and scored for size and signal intensity, presence of soft tissue hyperintensity, and bony expansion or collapse (in the spine) as shown in Figure 1, Figure 2, and Figure 3. These were further graded/scored as shown in the data collection sheet in Supplementary Table 1 (available with the online version of this article). The worst/highest signal intensity of bone marrow was recorded in the area of involvement/or the given bone segment as shown in Figure 1. The scoring of signal size was conducted based on the percentage of the whole segment of bone evaluated on the images after reviewing all images by scrolling back and forth on PACS.

Clinical assessment. There are no standard or specific outcome measures to assess the clinical disease burden in patients with CNO. In this study, all patients were evaluated for bony tenderness and swelling and the number of affected CNO sites was recorded. All available surrogate clinical outcome



Figure 1. Grading of severity of different items used for assessment of CNO lesions of long tubular bones. The items (bone marrow signal size, signal intensity, adjacent soft tissue high signal, and bone expansion) were analyzed using the proposed grading system. Coronal T2 STIR images obtained through the distal tibiae in 5 different patients are shown. (A) A 13-year-old boy with no bone marrow signal changes resulting in a bone marrow signal size score of 0. (B) A 10-year-old girl with bone marrow signal size scored as grade 1 (< 25 % of distal epimetaphysis segment of the tibia). (C) An 11-year-old girl with bone marrow signal size scored as grade 2 (25–49% of epimetaphysis). (D) A 12-year-old boy with bone marrow signal size scored as grade 3 (50–74% of epimetaphysis). (E) A 9-year-old girl with bone marrow signal size scored as grade 4 (75–100% of epimetaphysis). The worst signal intensity of the involved bone segment was taken into consideration for the grading of signal intensity of the lesion as depicted in panels C and E, where marrow signal intensity is equal to the signal of the adjacent ankle joint fluid and hence scored as grade 2. Note the presence of surrounding soft tissue high signal received a grade of 1 in panels D and E. Hence the following scores were obtained: (A) 0; (B) 1; (C) 2 + 2 = 4; (D) 3 + 1 = 4; (E) 4 + 2 + 1 = 7. CNO: chronic nonbacterial osteomyelitis; STIR: short-tau inversion recovery.

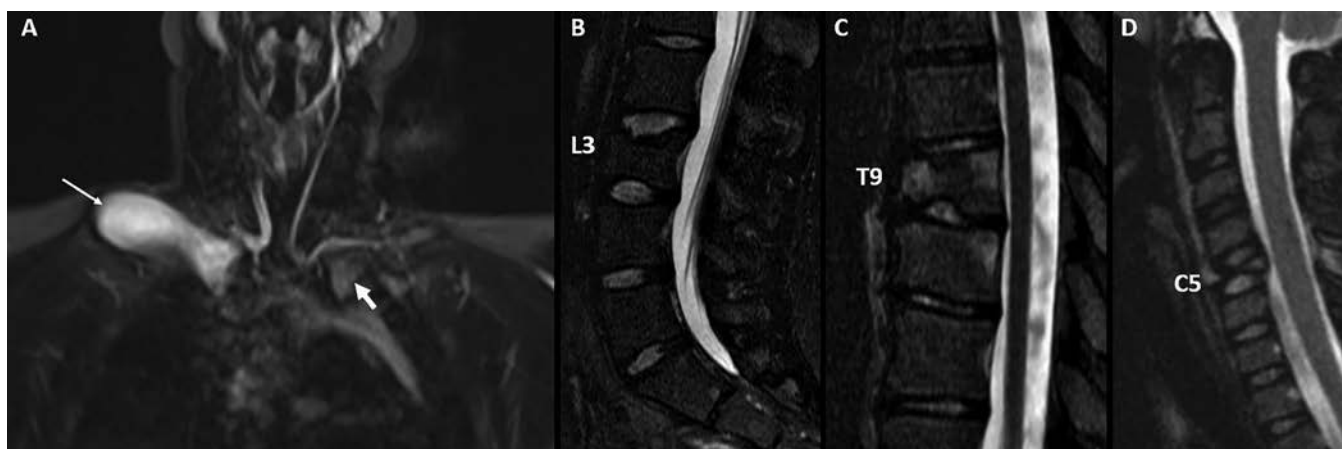


Figure 2. Presence of bone expansion and bone collapse. (A) Coronal T2 STIR image through the neck and chest in a 14-year-old boy with CNO demonstrates diffuse confluent marrow high signal and expansion of the medial half of right clavicle (long arrow) as compared to the normal contralateral clavicle (short arrow); accumulated an additional score of 1. (B–C) Sagittal T2 STIR images of the thoraco-lumbar spine in a 15-year-old boy show < 50% collapse of the L3 vertebra received a score of 1 whereas > 50% collapse of the involved T9 vertebra (mainly in the central part) received a score of 2. (D) Sagittal T2 STIR image of the cervical spine in a 6-year-old girl demonstrates completely flattened C5 vertebra (vertebra plana) receiving a score of 3. CNO: chronic nonbacterial osteomyelitis; STIR: short-tau inversion recovery.

measures were retrieved and analyzed pre- and posttreatment, which included presence or absence of bone pain, localized swelling, arthritis, rash, enthesitis, uveitis, systemic symptoms (fever, weight loss, fatigue, and gastrointestinal symptoms), and visual analog scale (VAS) score for pain. Laboratory variables including serum calcium, alkaline phosphatase, C-reactive protein, erythrocyte sedimentation rate, serum C-telopeptide (ng/L), and bisphosphonate treatment with pamidronate details were recorded as shown in Supplementary Table 2 (available with the online version of this article).

Statistical analysis. Descriptive analysis was performed to assess the

prevalence of CNO lesions at each proposed anatomical region. Any bone region (defined as per Supplementary Table 1, available with the online version of this article) to which a score of ≥ 1 was given by either of the 2 observers on the first pretreatment WB-MRI of the patient was counted to provide a sensitive estimate of the relative distribution of lesions. For assessment of detection of lesions, the interreader agreement was calculated using kappa coefficient (κ), by dichotomizing the 0–4 and 0–2 ordinal grades to 0 and 1, collapsing all nonzero grades. For the quantification of the lesion, the interreader agreement was conducted on the nonzero grades using κ statistics. The interrater reliability was considered excellent if the κ

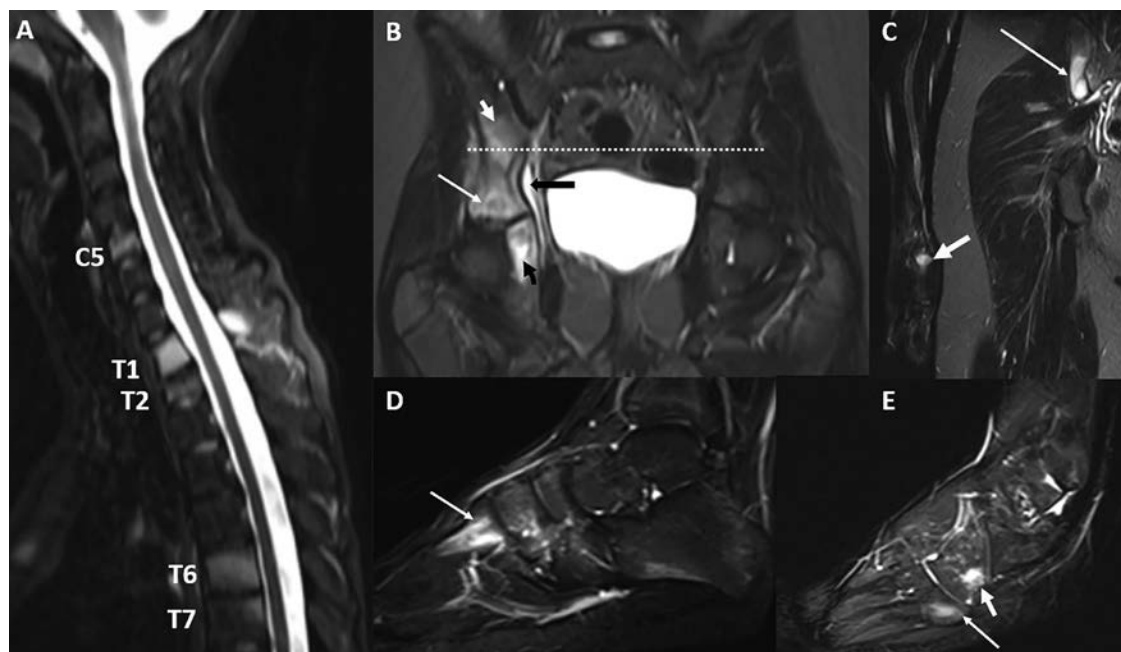


Figure 3. Examples of grading of different body regions for assessment of CNO lesion in different patients. (A) Sagittal T2 STIR image of the cervicothoracic spine in a 13-year-old girl shows multifocal vertebral involvement. Scores for C5 (SS + SI + C + PE = 4 + 1 + 0 + 0) = 5; T1 (4 + 2 + 0 + 1) = 7; T2 (4 + 1 + 1 + 0) = 6; T6 (4 + 1 + 0 + 0) = 5; and T7 (1 + 1 + 0 + 0) = 2. (B) Coronal T2 STIR image of the pelvis in an 11-year-old girl shows a score of 7 (SS + SI + ST + BE = 4 + 2 + 1 + 0) for the right-sided periacetabular lesion. Signal intensity (small black arrow) which is equal to the fluid in the urinary bladder received a score of 2 whereas presence of soft tissue hyperintensity (long black arrow) received a score of 1. The dotted line shows the watershed border between the iliac and periacetabular regions. Thus, the right iliac lesion received a score of 4 (i.e., 2 + 1 + 1 + 0). (C) Coronal T2 STIR image in a 15-year-old girl depicts presence of focal marrow hyperintensity in the first metacarpal (short white arrow) and received a score of 1. Note that the iliac bone lesion (long white arrow) is also seen in the same patient. (D–E) Sagittal images through the right foot in a 15-year-old boy received a score of 3 for the 3 involved bones. The other items were not recorded for small bones of feet and hand. BE: bone expansion; C: collapse; CNO: chronic nonbacterial osteomyelitis; PE: posterior element; SI: signal intensity; SS: signal size; ST: soft tissue; STIR: short-tau inversion recovery.

was > 0.80, good if it was 0.61–0.80, moderate if 0.41–0.60, and poor if ≤ 0.40. A bootstrapping method with 1000 resampling iterations was used to determine the 95% CI for the κ coefficients. Correlation between the bone lesion signal size and signal intensity was calculated using Spearman correlation coefficients.

Responsiveness was calculated using standardized response mean (SRM), defined as the mean change score over the SD of change score. The 2 scores from the 2 readers were averaged for each WB-MRI evaluation for pre- and posttreatment WB-MRI scores. All available treatment intervals of each patient were included for analysis. The absolute value of SRM was interpreted as large effect if > 0.8, moderate effect if 0.8–0.5, small effect if 0.5–0.2, and no effect if < 0.2. Data analysis was performed using the SPSS version 23.0 (IBM Corp.). In all analyses, P values < 0.05 were considered statistically significant.

RESULTS

Thirty-two patients were included in this study and baseline characteristics are summarized in Supplementary Table 2 (available with the online version of this article). The VAS score for pain was available for 19 of the 32 patients before and after their first cycle of pamidronate treatment. Median VAS score for pain pretreatment was 3.6 (IQR 0.7–5.6) and posttreatment was 0.9 (IQR 0.1–3.8). The median within-patient change in the VAS score was –1.0 (IQR –3.7 to 0.0), corresponding to a SRM of –0.52, indicating moderate effect size. Twenty-one (66%)

patients received 1 cycle of pamidronate, 8 patients received 2 cycles, and 2 and 1 patients received third and fourth cycles, respectively, because of persistent symptomatic extensive disease including spinal lesions. Pre- and posttreatment WB-MRI examinations were obtained after each cycle in all except 6 patients (3 pre- and posttreatment MRI were available in 5 patients who had 2 cycles and 5 MRI in 1 patient with 3 cycles of pamidronate) as described in Supplementary Figure 1 (available with the online version of this article). Thirty-one patients (96.9%) underwent a trial of NSAID as initial therapy, 6 patients (18.8%) received a short course of corticosteroid at initial presentation before confirmation of diagnosis. Three patients (9.4%) had a trial of biologic therapy for suspected juvenile idiopathic arthritis (JIA) before CNO diagnosis, and 3 (9.4%) others received disease-modifying antirheumatic drugs (DMARD). The results are reported below in 3 parts: (1) prevalence of lesions; (2) reliability of MRI assessment scoring system; and (3) MRI responsiveness to pamidronate therapy. Treatment response was assessed separately according to 1, 2, 3, and 4 pamidronate cycles in 32, 11, 3, and 1 patient, respectively. Ten patients (31%) with radiological evidence of persistent disease or presence of disease flare were started on a TNF blocker (8 on ADA and 2 on ETN) after the follow-up MRI. One additional patient was commenced on ETN for associated JIA.

Prevalence of lesions. Most lesions demonstrated multifocal ill-defined bone marrow hyperintensity on STIR images and were typically situated in the metaphyseal and epiphyseal regions adjacent to a growth plate of tubular bones. On WB-MRI STIR sequences, a total of 387 bone lesions (including 108 hand and feet bone lesions) were detected in 32 patients on baseline MRI examinations, before treatment with pamidronate. Lower limb regions were most commonly affected and occurred, in descending order, in the distal tibial metaepiphysis (66%), proximal tibial metaepiphysis (50%), distal femur metaepiphysis (50%), and distal fibular metaepiphysis (31%). Upper extremity involvement was considerably less common, affecting the distal ulnar and radial metaepiphysis in 20%. Among the axial sites, the sacrum (33%) was the most commonly affected site. The spine, clavicle, mandible, skull, sternum, and ribs were also involved to a variable extent. There was only 1 case of isolated coccygeal and ulnar diaphyseal involvement, whereas no lesions were found in the fibular and radial diaphysis and proximal radial metaepiphysis within this cohort. The detailed distribution of lesions is shown in Supplementary Table 3 (available with the online version of this article).

High signal intensity within the surrounding soft tissues was observed in 47 lesions on the baseline studies (Supplementary Table 3, available with the online version of this article), predominantly adjacent to tubular bones of lower limbs (26 of 640 locations examined in the legs), followed by pelvis (particularly along the periacetabular region), clavicle, mandible, and spine. The bony expansion was present in 11 studied regions in baseline WB-MRI and typically seen with clavicle and mandible. The bone collapse in the spine was commonly seen in the thoracic spine (3 of 9 involved thoracic vertebrae).

Reliability of MRI assessment of lesions. For the detection of the lesions, interreader agreement on the detection of bone marrow lesions was excellent for all the body regions, with κ ranging from 0.93 to 1.00, as shown in Table 1. Soft tissue changes and bone expansion or collapse were too infrequently observed in this sample to estimate interreader agreement. Interreader reliability of detection of bone marrow lesions, soft tissue lesions, bone expansion or collapse (in the spine), and posterior element

involvement (in spine lesion) scores were assessed based on the images from the first pretreatment MRI of 32 patients. CIs are derived from 1000 bootstrap resamplings. A lesion was counted if either of the 2 readers rated the bone region as nonzero for the specific finding.

For the quantification of the lesions, there was excellent interreader agreement on both the quantification of size and signal intensity of bone lesions in the arms and legs. There was perfect agreement on the size quantification of bone lesions in the pelvis, but moderate agreement on the signal intensity assessment (Table 1). Perfect agreement was observed for both size and intensity in the 18 spine lesions observed. Perfect agreement was observed in the size of lesions in the shoulder girdle, with good agreement on signal intensity. Lesion counts were low in the head and thorax in these patients, precluding more precise agreement estimates.

Responsiveness of MRI-detected lesions to pamidronate. Response to pamidronate therapy was quantified for the first pamidronate cycle for all 32 patients using SRM of the change in the size and intensity of the bone lesion signal, separated by the body region. The majority of the bone marrow lesions were seen in the upper and lower limbs and pelvis. After the first cycle of pamidronate, both the signal size and intensity of these lesions showed a small response to therapy in the shoulder girdle and the lower limb lesions, whereas in lesions of the upper limb and pelvis, the treatment response was not significant for either of these features. Lesions in the spine showed the highest response to treatment (Figure 4), at a decrease of 0.987 SRM for the signal size and 0.922 for signal intensity for the 20 lesions studied (Table 2). Responsiveness was high also in the skull and thorax, although the number of observed lesions was low in these regions. After the first cycle, 96 of the 279 lesions resolved (34%), whereas in the subset of 11 patients who underwent 2 or more cycles, 76% of lesions resolved after the second cycle. Twenty-one (7.5%) lesions worsened and 46 (16.4%) new lesions developed after 1 cycle (in all 32 patients); the number of worsened lesions reduced to 2 (2%) and new lesions to 14 (14.9%) after the second cycle in 11 patients (Supplementary Table 4, available with the online version of this article).

Table 1. Interreader agreement on the detection and assessment of the size and signal intensity of bone marrow lesions on the first pretreatment MRI of 32 pediatric patients with CNO.

	No. Regions Examined		Bone Marrow Lesions, κ (95% CI)			Soft Tissue Hyperintensity		Bone Expansion/Collapse ^a	
	N		Presence	Signal Size	Signal Intensity	N	κ (95% CI)	N	κ (95% CI)
Head	128	6	1.00 (1.00–1.00)	0.76 (.36–1.00)	0.57 (0.00–1.00)	2	1.00 (1.00–1.00)	2	0.80 (0.00–1.00)
Shoulder girdle	128	13	0.96 (0.85–1.00)	0.88 (0.56–1.00)	0.60 (0.18–1.00)	4	1.00 (1.00–1.00)	3	1.000 (1.00–1.00)
Thorax	96	4	1.00 (1.00–1.00)	–	0.00 (–0.60–1.00)	0	–	0	–
Pelvis	288	45	0.97 (0.94–1.00)	0.92 (0.79–1.00)	0.47 (0.21–0.70)	7	0.75 (0.00–1.00)	1	0.50 (0.00–1.00)
Upper limbs	576	38	0.93 (0.86–0.99)	0.65 (0.44–0.83)	0.61 (0.36–0.82)	1	1.00 (1.00–1.00)	1	1.00 (1.00–1.00)
Lower limbs	640	155	0.98 (0.96–1.00)	0.80 (0.71–0.87)	0.75 (0.64–0.85)	26	0.82 (0.66–0.93)	4	0.72 (0.33–1.00)
Spine	768	18	0.97 (0.90–1.00)	0.88 (0.63–1.00)	0.83 (0.29–1.00)	2	1.00 (1.00–1.00)	5	0.80 (0.00–1.00)

^a Bone collapse is measured for spine, whereas bone expansion is measured for other regions. CNO: chronic nonbacterial osteomyelitis; MRI: magnetic resonance imaging.

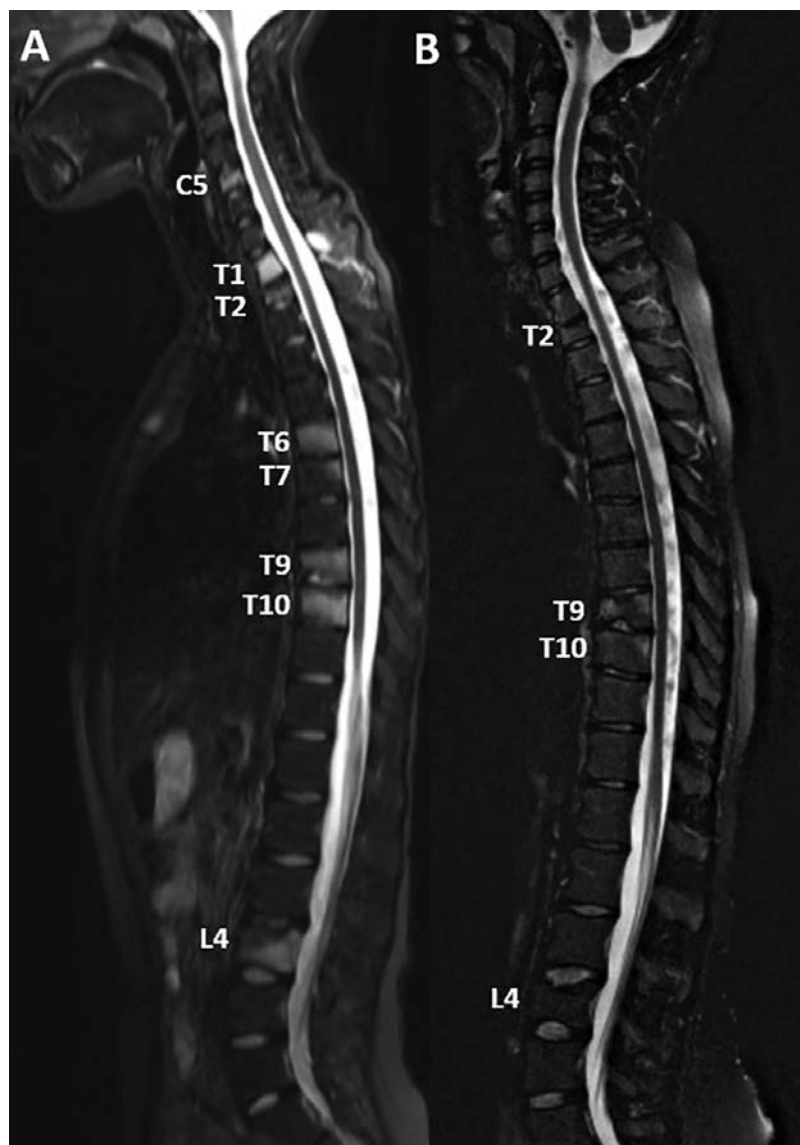


Figure 4. Pre- and postpamidronate WB-MRI in a 15-year-old boy with CNO. (A) Sagittal STIR whole spine image before pamidronate therapy shows marrow high signal involving the C5, T1, T2, T6, T7, T9, T10, and L1 vertebral bodies consistent with vertebral lesions. The total score of the vertebral lesions dropped from 45 to 11 after 1 cycle of pamidronate was administered to patients as seen on posttreatment STIR sagittal spine image. (B) Consistent with considerable response to treatment. CNO: chronic nonbacterial osteomyelitis; STIR: short-tau inversion recovery; WB-MRI: whole-body magnetic resonance imaging.

DISCUSSION

CNO is a painful, autoinflammatory osteitis, which may have a protracted course over the years, and is managed using a variety of treatments including NSAID, nonbiologic DMARD, corticosteroids, bisphosphonates, and biologic agents. Previously, bisphosphonates have shown effective and rapid pain relief in pediatric patients with persistent CNO, including improvement of bone lesions on serial MRI²⁸. Bisphosphonates act as analgesic agents inhibiting bone resorption and have antiinflammatory properties as well³⁷. They have been used in adults and children in many bone disorders associated with significant osteopenia³⁸.

Our study presented data on interreader agreement on the

detection and quantification of bone lesions and MRI response to pamidronate in pediatric patients with CNO with ongoing disease activity despite antiinflammatories. CNO lesions are most frequently seen to involve the metaepiphysis of tubular bones, pelvic bones, small bones of feet, spine, and clavicles in the present study, and this is in agreement with previous studies^{14,39,40,41}. This study examined the efficacy of pamidronate by comparing the pre- and post-WB-MRI bone lesions in pediatric patients with CNO. Overall, pamidronate therapy led to a good response (using WB-MRI as an objective measurement of disease activity) with the resolution of the bony lesions on follow-up MRI in 34% and 76% after 1 and 2 cycles of pamidronate therapy, respectively. This is in concordance with

Table 2. Response to the treatment in axial and appendicular lesions in 32 patients during first cycle of pamidronate as measured by WB-MRI.

Bone Region	Total Locations Examined	Lesion Signal Size		Lesion Signal Intensity	
		No. of Involved Locations in Pre-/Post-Treatment	SRM	No. of Involved Locations in Pre-/Post-Treatment	SRM
Head (skull, mandible)	128	6	−0.645	6	−0.598
Shoulder girdle (clavicle, scapula)	128	16	−0.412	16	−0.530
Thorax (sternum, ribs)	800	4	−0.866	4	−1.095
Pelvis (hip bones, sacrum, coccyx)	288	59	−0.193	59	−0.019
Arms (humerus, radius, ulna)	576	54	−0.194	54	−0.341
Legs (femur, tibia, fibula)	640	183	−0.325	183	−0.244
Spine (C1–L5 vertebrae)	768	20	−0.987	20	−0.922

Bone Region	Total Hands/Feet Examined	No. of Hands/Feet With ≥ 1 Lesion in Pre-/Post-treatment MRI		SRM
Hand ^a	64	4		−0.614
Foot ^a	64	45		−0.210

^a The response to hand and foot bone lesions is mentioned separately because the hand and foot lesions were not tracked per lesion over time in contrast to the other lesions. SRM: standardized response mean. WB-MRI: whole-body magnetic resonance imaging.

prior studies that demonstrated a similar response to pamidronate treatment^{27,28,30}. Although 34% of lesions disappeared after 1 cycle of treatment, ongoing improvement with a substantial response (resolution of 76% of the lesions) noted on WB-MRI occurred after 2 cycles in 11 patients. Twenty-one patients had only 1 cycle of therapy with overall > 50% of residual and 16% of new lesions being noted on WB-MRI despite good clinical response. These results highlight the importance of using WB-MRI in assessing subclinical disease and response to treatment, which can help guide in treatment decisions. In the group of patients who received > 1 cycle of pamidronate treatment, some lesions resolved/disappeared in between the cycles, as evident on pretreatment MRI examinations for the next cycle, once again emphasizing the role of WB-MRI in quantifying CNO lesions.

Our study proposes a new MRI scoring tool for CNO lesions and shows excellent interreader reliability for detecting and quantifying the size of the CNO lesions conversely to signal intensity of the bone marrow lesion. In our study, the signal intensity of the lesion was less reliable than size, as the grading of the signal was quite variable among readers and depended upon the windowing of the image while evaluating on PACS. To our knowledge, there is no prior study available in the literature against which the results of our study could be compared concerning the intensity of bone marrow edema in assessing CNO lesions. Hence, this point should be further evaluated in future prospective studies. Lesions in the bones of the feet were more common than in the hand, which is in keeping with the predilection of disease to involve the lower limb. However, it could have been affected by the visibility/readability of lesions on WB-MRI. Dedicated sagittal STIR sequences separately for the right and left foot were included in our WB-MRI CNO protocol; however, hands were imaged as a part of coronal STIR station 3 (through the lower abdomen and pelvis) and seen at the periphery of the image. Hence, we may have missed

lesions in this region due to poor visualization of bones of the hand.

In our cohort, spinal lesions showed an excellent response to pamidronate with SRM of 0.9, which is consistent with prior published studies that have found the almost equal efficacy of pamidronate to spinal disease^{28,29,30,42,43,44}.

There were several limitations in our study. First, it is a retrospective study that may result in missing clinical details that were not acquired in a standardized manner, including VAS score for pain. Second, there could have been the effect of initial non-pamidronate treatment (NSAID, DMARD, steroids, and biologics) on treatment outcomes. Further, interobserver variability in quantifying the intensity of bone marrow edema of the lesions was suboptimal and could be improved in future by the utilization of an atlas to guide scoring. In addition, during certain stages of skeletal maturation linear bands of increased STIR signal intensity are noted at the metaphysis of the long bones as part of a physiologic process. This information could be made available in an atlas to avoid false-positive scoring in future studies. The lack of dedicated hand imaging in our protocol likely led to the underestimation of bone lesions in this location, and can be addressed in future prospective studies by placing the hands on thighs for better visibility. This study also did not correlate the radiologic changes with clinical variables of disease activity.

In this study, the interobserver reliability for detecting pediatric CNO lesions on MRI was excellent. When experienced radiologists report MRI data on CNO, we can be confident that the detailed assessment of MRI for these bone lesions is reproducible. On the other hand, further tutorial tools should be developed to improve the reliability of assessment of the signal intensity of CNO lesions. Nevertheless, MRI is an important and clinically relevant quantification tool that can be used to determine disease activity, extent of disease (including disease sites that may be clinically occult), monitor treatment response, make treatment adjustments, and perform follow-up examinations.

ONLINE SUPPLEMENT

Supplementary material accompanies the online version of this article.

REFERENCES

1. Surendra G, Shetty U. Chronic recurrent multifocal osteomyelitis: a rare entity. *J Med Imaging Radiat Oncol* 2015;59:436-44.
2. Ferguson PJ, El-Shanti HI. Autoinflammatory bone disorders. *Curr Opin Rheumatol* 2007;19:492-8.
3. Iyer RS, Thapa MM, Chew FS. Chronic recurrent multifocal osteomyelitis: review. *AJR Am J Roentgenol* 2011;196:S87-91.
4. Carr AJ, Cole WG, Robertson DM, Chow CW. Chronic multifocal osteomyelitis. *J Bone Joint Surg Br* 1993;75:582-91.
5. Schultz C, Holterhus PM, Seidel A, Jonas S, Barthel M, Kruse K, et al. Chronic recurrent multifocal osteomyelitis in children. *Pediatr Infect Dis J* 1999;18:1008-13.
6. Beretta-Piccoli BC, Sauvain MJ, Gal I, Schibler A, Saurenmann T, Kressebuech H, et al. Synovitis, acne, pustulosis, hyperostosis, osteitis (SAPHO) syndrome in childhood: a report of ten cases and review of the literature. *Eur J Pediatr* 2000;159:594-601.
7. Omid CJ, Siegfried EC. Chronic recurrent multifocal osteomyelitis preceding pyoderma gangrenosum and occult ulcerative colitis in a pediatric patient. *Pediatr Dermatol* 1998;15:435-8.
8. Laxer RM, Shore AD, Manson D, King S, Silverman ED, Wilmot DM. Chronic recurrent multifocal osteomyelitis and psoriasis--a report of a new association and review of related disorders. *Semin Arthritis Rheum* 1988;17:260-70.
9. Vittecoq O, Said LA, Michot C, Mejjad O, Thomine JM, Mitrofanoff P, et al. Evolution of chronic recurrent multifocal osteitis toward spondylarthropathy over the long term. *Arthritis Rheum* 2000;43:109-19.
10. Demharter J, Bohndorf K, Michl W, Vogt H. Chronic recurrent multifocal osteomyelitis: a radiological and clinical investigation of five cases. *Skeletal Radiol* 1997;26:579-88.
11. Roderick MR, Ramanan AV. Chronic recurrent multifocal osteomyelitis. *Adv Exp Med Biol* 2013;764:99-107.
12. Costa-Reis P, Sullivan KE. Chronic recurrent multifocal osteomyelitis. *J Clin Immunol* 2013;33:1043-56.
13. Němcová D, Košková E, Macku M, Brejchová I, Hoza J, Schiller M, et al. Chronic recurrent multifocal osteomyelitis (CRMO): clinical features and outcome in 21 Czech and Slovak children. *Clin Exp Rheumatol* 2011;29:391.
14. Khanna G, Sato TSP, Ferguson P. Imaging of chronic recurrent multifocal osteomyelitis. *Radiographics* 2009;29:1159-77.
15. Mandell GA, Contreras SJ, Conard K, Harcke HT, Maas KW. Bone scintigraphy in the detection of chronic recurrent multifocal osteomyelitis. *J Nucl Med* 1998;39:1778-83.
16. Fritz J, Tzaribatchev N, Claussen CD, Carrino JA, Horger MS. Chronic recurrent multifocal osteomyelitis: comparison of whole-body MR imaging with radiography and correlation with clinical and laboratory data. *Radiology* 2009;252:842-51.
17. Girschick HJ, Raab P, Surbaum S, Trusen A, Kirschner S, Schneider P, et al. Chronic non-bacterial osteomyelitis in children. *Ann Rheum Dis* 2005;64:279-85.
18. Jansson A, Renner ED, Ramser J, Mayer A, Haban M, Meindl A, et al. Classification of non-bacterial osteitis: retrospective study of clinical, immunological and genetic aspects in 89 patients. *Rheumatology* 2007;46:154-60.
19. Job-Deslandre C, Krebs S, Kahan A. Chronic recurrent multifocal osteomyelitis: five-year outcomes in 14 pediatric cases. *Joint Bone Spine* 2001;68:245-51.
20. Kerrison C, Davidson JE, Cleary AG, Beresford MW. Pamidronate in the treatment of childhood SAPHO syndrome. *Rheumatology* 2004;43:1246-51.
21. Schnabel A, Range U, Hahn G, Berner R, Hedrich CM. Treatment response and longterm outcomes in children with chronic nonbacterial osteomyelitis. *J Rheumatol* 2017;44:1058-65.
22. Carpenter E, Jackson MA, Friesen CA, Scarbrough M, Roberts CC. Crohn's-associated chronic recurrent multifocal osteomyelitis responsive to infliximab. *J Pediatr* 2004;144:541-4.
23. Guérin-Pfiffer S, Guillaume-Czitrom S, Tammam S, Koné-Paut I. Evaluation of chronic recurrent multifocal osteitis in children by whole-body magnetic resonance imaging. *Joint Bone Spine* 2012;79:616-20.
24. Darge K, Jaramillo D, Siegel MJ. Whole-body MRI in children: current status and future applications. *Eur J Radiol* 2008;68:289-98.
25. Merlini L, Carpentier M, Ferrey S, Anooshiravani M, Poletti P-A, Hanquinet S. Whole-body MRI in children: would a 3D STIR sequence alone be sufficient for investigating common paediatric conditions? A comparative study. *Eur J Radiol* 2017;88:155-62.
26. Zhao Y, Chauvin NA, Jaramillo D, Burnham JM. Aggressive therapy reduces disease activity without skeletal damage progression in chronic nonbacterial osteomyelitis. *J Rheumatol* 2015;42:1245-51.
27. Roderick M, Shah R, Finn A, Ramanan AV. Efficacy of pamidronate therapy in children with chronic non-bacterial osteitis: disease activity assessment by whole body magnetic resonance imaging. *Rheumatology* 2014;53:1973-6.
28. Miettinen PM, Wei X, Kaura D, Reslan WA, Aguirre AN, Kellner JD. Dramatic pain relief and resolution of bone inflammation following pamidronate in 9 pediatric patients with persistent chronic recurrent multifocal osteomyelitis (CRMO). *Pediatr Rheumatol Online J* 2009;7:2.
29. Hofmann C, Wurm M, Schwarz T, Neubauer H, Beer M, Girschick H, et al. A standardized clinical and radiological follow-up of patients with chronic non-bacterial osteomyelitis treated with pamidronate. *Clin Exp Rheumatol* 2014;32:604-9.
30. Bhat CS, Roderick M, Sen ES, Finn A, Ramanan A. Efficacy of pamidronate in children with chronic non-bacterial osteitis using whole body MRI as a marker of disease activity. *Pediatr Rheumatol Online J* 2019;17:35.
31. Zhao Y, Sato TS, Nielsen SM, Beer M, Huang M, Iyer RS, et al. Development of CROMRIS (Chronic nonbacterial Osteomyelitis MRI Scoring) tool and evaluation of its interrater reliability. *J Rheumatol* 2019;47:190186.
32. Andreasen CM, Jurik AG, Glerup MB, Høst C, Mahler BT, Hauge E-M, et al. Response to early-onset pamidronate treatment in chronic nonbacterial osteomyelitis: a retrospective single-center study. *J Rheumatol* 2019;46:1515-1523.
33. Ramanan AV, Roderick MR, Shah R, Finn A. A75: Proposal of the Bristol Criteria for the diagnosis of chronic non-bacterial osteitis from a cohort of 41 patients. *Arthritis Rheumatol* 2014;66:S107.
34. Roderick MR, Shah R, Rogers V, Finn A, Ramanan AV. Chronic recurrent multifocal osteomyelitis (CRMO) - advancing the diagnosis. *Pediatr Rheumatol Online J* 2016;14:47.
35. Maksymowych WP, Inman RD, Salonen D, Dhillon SS, Williams M, Stone M, et al. Spondyloarthritis Research Consortium of Canada magnetic resonance imaging index for assessment of sacroiliac joint inflammation in ankylosing spondylitis. *Arthritis Rheum* 2005;53:703-9.
36. Panwar J, Tse S, Lim L, Tolend M, Radhakrishnan S, Salman M, et al. Spondyloarthritis Research Consortium of Canada) scoring system for sacroiliitis in juvenile spondyloarthritis/enthesitis-related arthritis: a reliability, validity, and responsiveness study. *J Rheumatol* 2019;46:636-44.
37. Drake MT, Clarke BL, Khosla S. Bisphosphonates: mechanism of action and role in clinical practice. *Mayo Clin Proc* 2008;83:1032-45.
38. Munns CF, Rauch F, Travers R, Glorieux FH. Effects of intravenous pamidronate treatment in infants with osteogenesis imperfecta: clinical and histomorphometric outcome. *J Bone Miner Res* 2005;20:1235-43.

39. Borzutzky A, Stern S, Reiff A, Zurakowski D, Steinberg EA, Dedeoglu F, et al. Pediatric chronic nonbacterial osteomyelitis. *Pediatrics* 2012;130:e1190-7.
40. Schnabel A, Range U, Hahn G, Siepmann T, Berner R, Hedrich CM. Unexpectedly high incidences of chronic non-bacterial as compared to bacterial osteomyelitis in children. *Rheumatol Int* 2016;36:1737-1745.
41. Girschick HJ, Zimmer C, Klaus G, Darge K, Dick A, Morbach H. Chronic recurrent multifocal osteomyelitis: what is it and how should it be treated? *Nat Clin Pract Rheumatol* 2007;3:733-738.
42. Wipff J, Costantino F, Lemelle I, Pajot C, Duquesne A, Lorrot M, et al. A large national cohort of French patients with chronic recurrent multifocal osteitis. *Arthritis Rheumatol* 2015;67:1128-37.
43. Hospach T, Langendoerfer M, von Kalle T, Maier J, Dannecker GE. Spinal involvement in chronic recurrent multifocal osteomyelitis (CRMO) in childhood and effect of pamidronate. *Eur J Pediatr* 2010;169:1105-11.
44. Gleeson H, Wiltshire E, Briody J, Hall J, Chaitow J, Sillence D, et al. Childhood chronic recurrent multifocal osteomyelitis: pamidronate therapy decreases pain and improves vertebral shape. *J Rheumatol* 2008;35:707-12.